STABILITY RELATIONS OF ALUMINUM HYDROXY-FLUORIDE HYDRATE, A RALSTONITE-LIKE MINERAL, IN THE SYSTEM AlF$_3$–Al$_2$O$_3$–H$_2$O–HF

Philip E. ROSENBERG[§]

Department of Geology, Washington State University, Pullman, Washington 99164–2812, U.S.A.

Abstract

Phase relations in the system AlF$_3$–Al$_2$O$_3$–H$_2$O–HF have been investigated between 400° and 700°C using sealed gold tubes and conventional hydrothermal techniques. Stable crystalline assemblages synthesized include (1) Al$_2$F$_{6-y}$(OH)$_y$•nH$_2$O (pyrochlore structure) + corundum (or diaspore), (2) Al$_2$F$_{6-y}$(OH)$_y$•nH$_2$O, (3) AlF$_{3-x}$(OH)$_x$ (α-AlF$_3$ structure) + Al$_2$F$_{6-y}$(OH)$_y$•nH$_2$O, 4) AlF$_2$(OH) (β-AlF$_3$ structure) + Al$_2$F$_{6-y}$(OH)$_y$•nH$_2$O, (5) AlF$_2$(OH) + corundum, (6) AlF$_2$(OH) + AlF$_{3-x}$(OH)$_x$, (7) AlF$_{3-x}$(OH)$_x$ + corundum, and (8) AlF$_{3-x}$(OH)$_x$. Compositions of solids were determined using XRD methods after calibration with results of electron-microprobe analyses. The maximum thermal stability of Al$_2$F$_{6-y}$(OH)$_y$•nH$_2$O is 575°C in assemblages with AlF$_2$(OH) or corundum, and 435°C in the presence of AlF$_{3-x}$(OH)$_x$. AlF$_2$(OH) replaces Al$_2$F$_{6-y}$(OH)$_y$•nH$_2$O in assemblages synthesized above these temperatures and, in turn, decomposes to AlF$_{3-x}$(OH)$_x$ above 625°C. Al$_2$F$_{6-y}$(OH)$_y$•nH$_2$O hydrolyzes with decreasing temperature in the F-deficient portion of the system and with increasing temperature in the F-rich portion of the system, with the result that the range of Al$_2$F$_{6-y}$(OH)$_y$•nH$_2$O compositions on the join AlF$_3$–Al(OH)$_3$ contracts from almost 15 mol.% Al(OH)$_3$ at 400°C to a single composition, 58 mol.% Al(OH)$_3$, at 575°C.

Keywords: volcanic emissions, fumarolic deposits, aluminum fluoride synthesis, ralstonite-like mineral.

Sommaire

Les relations de phases du système AlF$_3$–Al$_2$O$_3$–H$_2$O–HF ont fait l'objet d'études entre 400° et 700°C par techniques hydrothermales conventionnelles et avec tubes en or scellés. Parmi les assemblages cristallins synthétiques stables, on trouve (1) Al$_2$F$_{6-y}$(OH)$_y$•nH$_2$O (structure de type pyrochlore) + corindon (ou diaspore), (2) Al$_2$F$_{6-y}$(OH)$_y$•nH$_2$O, (3) AlF$_{3-x}$(OH)$_x$ (structure de α-AlF$_3$) + Al$_2$F$_{6-y}$(OH)$_y$•nH$_2$O, 4) AlF$_2$(OH) (structure de β-AlF$_3$) + Al$_2$F$_{6-y}$(OH)$_y$•nH$_2$O, (5) AlF$_2$(OH) + corindon, (6) AlF$_2$(OH) + AlF$_{3-x}$(OH)$_x$, (7) AlF$_{3-x}$(OH)$_x$ + corindon, et (8) AlF$_{3-x}$(OH)$_x$. La composition des phases solides a été établie par diffraction X après calibrage faisant usage des résultats obtenus avec une microsonde électronique. Le maximum de stabilité thermique de Al$_2$F$_{6-y}$(OH)$_y$•nH$_2$O est 575°C dans les assemblages avec AlF$_2$(OH) ou corindon, et 435°C en présence de AlF$_{3-x}$(OH)$_x$. La phase AlF$_2$(OH) remplace Al$_2$F$_{6-y}$(OH)$_y$•nH$_2$O dans les assemblages synthésisés au delà de cette température et, à son tour, elle se décompose en AlF$_{3-x}$(OH)$_x$ au delà de 625°C. La phase Al$_2$F$_{6-y}$(OH)$_y$•nH$_2$O se hydrolyse à mesure que diminue la température dans la portion déficitaire en F du système, et avec une augmentation de la température dans la portion riche en F du système, avec comme résultat que l'intervalle de compositions de Al$_2$F$_{6-y}$(OH)$_y$•nH$_2$O dans le sous-système AlF$_3$–Al(OH)$_3$ diminue de presque 15% Al(OH)$_3$ (base molaire) à 400°C à une seule composition, 58% Al(OH)$_3$, à 575°C.

(Traduit par la Rédaction)

Mots-clés: émissions volcaniques, dépots fumerolliens, synthèse du fluorure d'aluminium, minéral de type ralstonite.

Introduction

Ralstonite-like minerals with the general formula Na$_x$Mg$_x$Al$_{2-x}$F$_{6-y}$(OH)$_y$•nH$_2$O, (pyrochlore structure; Pabst 1939), form an isostructural solid-solution series between aluminum hydroxy-fluoride hydrate ($x = 0$) and the Na- and Mg-rich end member ($x = 1$), ralstonite (Pauly 1965). The Na- and Mg-free end-member, Al$_{16}$(F,OH)$_{48}$•12–15H$_2$O (AHF), which occurs in nature (Desborough & Rostad 1980, Rosenberg 1988, Papike *et al.* 1991, Keith 1991, Africano & Bernard 2000) lies in the reciprocal ternary system AlF$_3$–Al$_2$O$_3$–H$_2$O–HF. Compositional variations and stability relations of AHF have been investigated in this study between 400 and 700°C (see also Rosenberg 1990).

Ralstonite and AHF have been observed in many fumarolic deposits (Naboko 1957, Naughton *et al.* 1976, Serafimova 1997, Birnie & Hall 1974, Carobbi & Cipriani 1951, Rosenberg 1988, Papike *et al.* 1991, Africano & Bernard 2000). Ralstonite-like minerals

---

have also been reported in miarolitic cavities in alkali granites, where they are considered to be among the last minerals to crystallize (Raade & Haug 1980), as a late hydrothermal replacement in carbonatite veins (Heinrich 1977) and alkali pegmatites (Kearns 1995), as well as in the Ivigtut cryolite deposit, in Greenland (Pauly 1965). They also can form as a product of the low-temperature alteration of basalt (Naughton *et al.* 1976) to rhyolitic (Desborough & Rostad 1980) rocks in acid, F-rich environments. At the Klyuchevskaya volcano in Kamchatka, Russia, ralstonite occurs as an alteration product of basalts produced by reactions with HF in volcanic gases at 200–300°C (Hitchon *et al.* 1976). However, ralstonite-like minerals may apparently be formed in any relatively low-temperature, acid, F-rich environment (Hitchon *et al.* 1976).

Although AHF is a rare mineral, it is of interest because it occurs in a specific geological environment. A knowledge of the stability relations of AHF may serve to place limits on environmental conditions during its formation.

PREVIOUS EXPERIMENTAL INVESTIGATIONS

AHF has been synthesized in previous studies, but little is known of its stability relations. Cowley & Scott (1948) precipitated AHF from solution at 100°C; they proposed a compositional range from $AlF_2(OH)$ to $AlF(OH)_2$. Grobelny (1977) synthesized AHF from supersaturated solutions at 100–150°C and pressures up to 20 atm., and extended its known compositional range to $AlF_{2.5}(OH)_{0.5}$. The AHF synthesized in these studies is hydrated, but it dehydrates at elevated temperatures and decomposes in air at 550°C (Grobelny 1977). Menz *et al.* (1992) obtained a composition of $AlF_{2.3}(OH)_{0.7} \cdot H_2O$. AHF has also been precipitated with cryolite from solutions at 25°C by Roberson & Hem (1968).

PROCEDURES

Experiments were conducted in the temperature range 400°–700°C at 2 kbar using sealed gold tubes and conventional hydrothermal techniques. Starting materials consisted of reagent-grade AlF_3 and recrystallized $Al(OH)_3$. These materials were mixed mechanically to make starting compositions with $AlF_3:Al(OH)_3$ molar values of 1:19, 1:9, 1:4, 1:2, 1:1, 2:1, 3:1, 4:1, and 9:1, to which distilled H_2O was added (solid/liquid ≥ 2/1). For most experiments, cold-seal vessels were quenched rapidly in cold water. Tubes were weighed to check for leaks before opening. For some experiments, quench pH was measured using a combination microelectrode (Microelectrodes Inc.). The duration of the experiments was 3 to 93 days.

Solid products were examined by optical microscopy, X-ray diffractometry and infrared spectroscopy. Variations in phase compositions were determined from characteristic X-ray measurements after electron-microprobe (EMP) calibration using AlF_3, recrystallized at 750°C, as a standard. The unit-cell dimensions of AHF were determined to within 0.002 Å by measurement of three X-ray reflections (Table 1; 311, 333, 440) against an internal standard (CdF_2). The extent of hydrolysis of $AlF_{3-x}(OH)_x$ was estimated by measurement of the (220) X-ray reflection at approximately 52.0° 2θ Cu$K\alpha$ against the same internal standard.

The presence and nature of (OH) and structural H_2O were investigated qualitatively by infrared spectroscopy. The samples were prepared using conventional KBr pellet techniques and run on a Beckman IR–8 infrared spectrophotometer with a blank KBr pellet in the reference beam.

PRODUCTS

Six solid phases were synthesized in the system AlF_3–Al_2O_3–H_2O–HF: $Al_2F_{6-y}(OH)_y \cdot nH_2O$ (AHF), $AlF_2(OH)$ (AFH), $AlF_{3-x}(OH)_x$ (A), "tohdite", $5Al_2O_3 \cdot H_2O$ (T), diaspore, AlO(OH) (Dsp), and corundum, Al_2O_3 (Crn) . Whereas the aluminum fluorides have specific compositions or ranges in composition, they are best characterized by structure type rather than chemical composition inasmuch as any given chemical composition may exist in more than one structural form. Three basic structure-types were observed here and elsewhere (*e.g.,* Grobelny 1977): (1) α-AlF_3, rhombohedral, (2) β-AlF_3, orthorhombic (pseudohexagonal), and (3) pyrochlore structure, cubic. Neither zharchikhite, $AlF(OH)_2$ (Jambor & Burke 1989), nor the F-bearing, gibbsite-like mineral, $Al(OH_{1-x}F_x)_3$ (Jambor *et al.* 1990), were synthesized in this study.

AHF

AHF, cubic (pyrochlore structure, Effenberger & Kluger 1984) was synthesized as clear crystals (cubes

TABLE 1. XRD DATA FOR AHF

hkl	This study* d_{obs}	This study* I/I_0	Hydrated** d_{obs}	Hydrated** I/I_0	Dehydrated** d_{obs}	Dehydrated** I/I_0	Natural*** d_{obs}	Natural*** I/I_0
111	5.64	100	5.72	100	5.70	100	5.72	100
220					3.44	7		
311	2.952	40	2.95	60	2.92	30	2.97	60
222	2.824	25	2.83	30	2.80	25	2.85	25
400	2.447	5	2.45	8	2.43	3	2.46	20
331	2.246	3	2.27	8	2.22	3		
422	1.999	10	1.99	20	1.98	28	2.01	10
333,511	1.885	20	1.88	35	1.86	30	1.899	15
440	1.732	15	1.73	35	1.71	25	1.743	20
531	1.657	5	1.65	10	1.63	15	1.667	5
620	1.551	3	1.54	8	1.53	5	1.563	3

* Table 2, sample 968.   ** Grobelny (1977).   *** Desborough & Rostad (1980).

and octahedra) usually 10–30 μm in size. XRD data for AHF synthesized in this and other studies are compared in Table 1; experimental results for AHF-bearing assemblages are summarized in Tables 2 and 3. The infrared spectrum of AHF in the OH-stretching region (Fig. 1) shows absorption bands at 3663, 3546 cm^{-1} corresponding to structural (OH), 3425 cm^{-1} corresponding to (OH) or H_2O, and bands at 2941 and 1605 cm^{-1}, suggesting the presence of H_2O.

The unit-cell dimensions of AHF (Tables 2, 3) vary directly with the hydration state and inversely with the F:Al ratio (Cowley & Scott 1948, Grobelny 1977). However, the (220) X-ray reflection is present only in dehydrated samples (Crowley & Scott 1948, Grobelny 1977). Inasmuch as this peak is invariably absent in AHF synthesized in this study (Table 1), all samples are assumed to be hydrated. Synthetic AHF varies between $n = 0.9$ and 1.0 (Grobelny 1977); most natural samples of ralstonite also lie within this range (Pabst 1939, Pauly 1965, Di Girolamo & Franco 1968).

The variation of the unit-cell dimension a of AHF with F:Al ratio was determined by EMP analyses of five samples (Table 2; 372, 373, 644, 680, 822). Regression analysis was used to define a linear relationship ($R^2 = 0.852$) between cell dimensions and the F content of AHF (Fig. 2), which provided an estimate of the compositions of AHF synthesized in this study (Tables 2, 3). At 400°C, compositions of synthetic AHF range from $AlF_{1.33} (OH)_{1.67}$ in assemblages with A and fluid to $AlF_{1.1}(OH)_{1.9}$ in assemblages with corundum and fluid. At 575°C, this range narrows to a single composition, $AlF_{1.7} (OH)_{1.3}$. The unit-cell dimension of AHF synthesized at 400°C varies from a minimum value of 9.780 Å in F-rich assemblages (Table 3) to a maximum value

of 9.827 Å in F-poor assemblages (Table 2). Similar unit-cell dimensions were reported by Cowley & Scott (1948) and by Grobelny (1977) for synthetic AHF, 9.83 and 9.85 Å, respectively.

AFH

AFH is a phase that is compositionally similar to AHF but structurally distinct; it has been synthesized as hexagonal prisms up to 100 μm in length. X-ray powder data for AFH are given in Table 4. The infrared spectrum of AFH in the OH-stretching region (Fig. 1) shows absorption bands at 3663 cm^{-1} corresponding to structural (OH), 3413 cm^{-1} corresponding to (OH) or H_2O, and bands at 2941 and 1605 cm^{-1}, suggesting the presence of H_2O.

AFH has been synthesized at temperatures as high as 650°C in experiments of short duration (*e.g.*, 3 days), but it decomposes above about 625°C to form A + Crn in experiments of longer duration (*e.g.*, 14 days). AFH has not been synthesized at temperatures below 450°C (Tables 3, 5 and 6). Thus, AFH appears to exhibit a minimum (435°C) as well as a maximum (625°C) thermal stability in the ternary system.

TABLE 2. EXPERIMENTAL DATA: AHF COEXISTING WITH AFH OR A AND FLUID

Temp. (°C)	Sample no.	Comp.* (+ H₂O)	Time (days)	Products (+ fluid)	a, AHF (Å)	F,AHF (wt.%)
575	820	4:1	10	AHF + AFH	9.792	30.0
	788	4:1	5	AHF + AFH	9.792	30.2
550	782	4:1	21	AHF + AFH	9.789	30.3
	766	9:1	19	AHF + AFH	9.788	30.4
500	848	9:1	14	AHF + AFH	9.788	30.4
	846	9:1	24	AHF + AFH	9.789	30.3
	813	4:1	8	AHF + AFH	9.787	30.5
	1290	A	7	AFH + AHF	nm	-
475	1399	9:1	93	AHF + AFH	9.785	30.7
450	964	4:1	24	AHF + AFH	9.783	30.9
	967	9:1	24	AHF + AFH	9.783	30.9
	1353	9:1	24	AHF + A	nm	-
	1354	A	24	A + AHF	nm	-
425	986	9:1	34	AHF + A	9.783	30.9
	985	A	34	AHF + A	9.781	31.1
	984	A	34	AHF + A	9.782	31.0
400	1029	9:1	40	AHF + A	9.780	31.2
	1031	A	40	A + AHF		nm

* AlF₃ : Al(OH)₃ molar ratio. A: AlF₃₋ₓ(OH)ₓ, F: fluorine content, nm: not measured.

TABLE 3. EXPERIMENTAL DATA: AHF ± Crn OR T

Temp. (°C)	Sample no.	Comp.* (+ H₂O)	Time (days)	Products (+ fluid)	a, AHF (Å)	F,AHF (wt.%)
575	822	1:9	10	AHF + T	9.792	30.0
565	855	1:4	21	AHF + Crn	9.793	29.9
	856	1:9	21	AHF + T	nm	-
	854	3:1	21	AHF	9.794	29.5
	853	2:1	21	AHF + Crn-m	9.792	30.0
550	767	3:1	19	AHF	9.794	29.5
	644	2:1	5	AHF + Crn-m	9.793	29.9
525	602	1:4	22	AHF + T	9.798	29.3
	601	2:1	22	AHF + Crn	9.804	28.6
	509	1:4	12	AHF + T	9.805	28.5
	510	2:1	12	AHF + Crn-m	9.799	31.3
520	322	1:4	35	AHF + T	9.805	28.5
	317	1:1	35	AHF + Crn	9.802	28.8
510	313	2:1	44	AHF + Ttr	9.805	28.5
	312	1:4	44	AHF + T	9.809	28.1
	314	1:2	44	AHF + T + Crn	9.811	27.9
500	506	2:1	12	AHF + Crn-m	9.804	28.6
	847	3:1	14	AHF	9.791	30.0
475	373	2:1	30	AHF + Crn-m	9.810	28.0
	372	1:4	30	AHF + T	9.807	28.3
	1400	1:19	93	T + AHF	nm	-
450	968	1:4	23	AHF + Crn-m	9.816	27.4
	963	3:1	23	AHF	9.792	30.0
	993	1:9	28	AHF + T	nm	-
	710	1:9	30	AHF + T	9.820	
	623	2:1	21	AHF + Crn-m	9.817	27.3
	624	1:4	21	AHF + T	9.818	27.2
	1360	1:19	24	T + AHF	nm	-
445	296	1:2	22	AHF + T	9.816	27.4
	295	1:1	22	AHF + Ttr	9.815	27.5
425	1336	1:4	92	AHF + T	nm	-
400	681	2:1	31	AHF	9.825	26.4
	680	1:4	31	AHF + Dsp	9.827	26.2
	730	1:9	33	Dsp + AHF	nm	-

* AlF₃ : Al(OH)₃ molar ratio. Symbols: AHF: Al₂F₆₋₃(OH)ₓ•nH₂O, Crn: corundum, T: "tohdite", Dsp: diaspore. Abbreviations: tr: X-ray trace, m: microscope only, a: unit-cell dimension, F: fluorine content, nm: not measured.
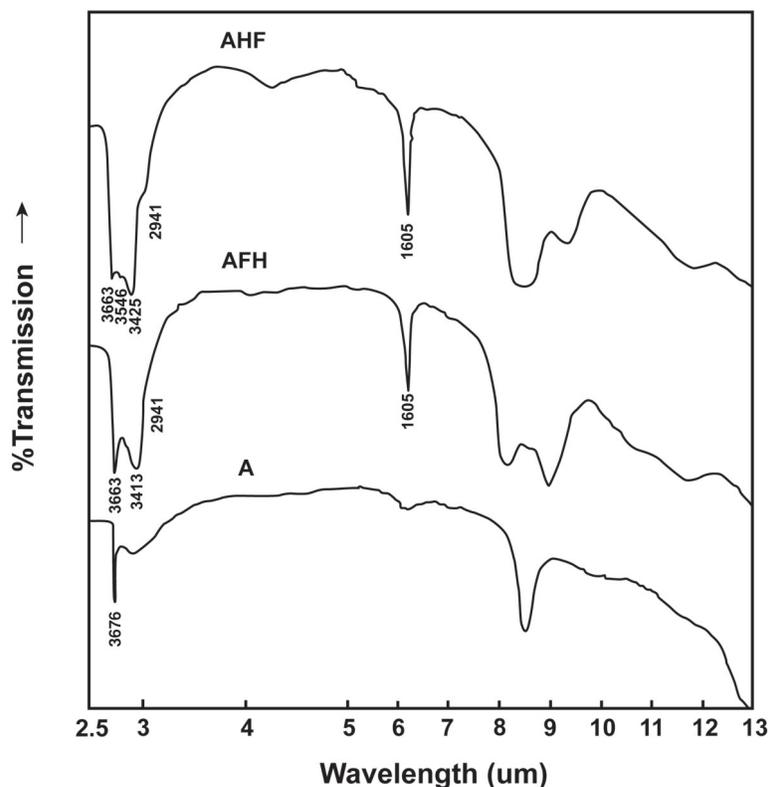
Fig. 1. Infrared absorption spectra of AHF, AFH and $AlF_{3-x}(OH)_x$. Absorption bands in cm^{-1}.
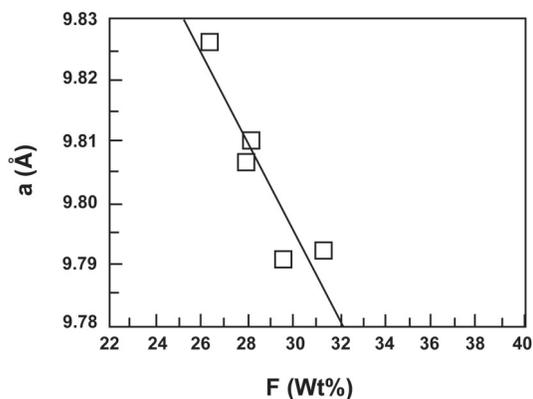
Fig. 2. Variation of AHF composition (wt.% F) with unit-cell dimension a. The size of the symbols approximates the estimated error.

The X-ray reflections of AFH (Table 4) were indexed assuming hexagonal symmetry. Calculated unit-cell dimensions are a 4.032(3), c 7.141(4) Å, V 100.58 Å^3, $Z = 2$. The calculated density is 2.71 g/cm^3, as compared to the measured density 2.72 g/cm^3. Routine X-ray measurements against an internal standard, CdF_2, showed only small variations in d values (Table 4). However, EMP analyses (46.3–43.0 wt.% F) indicate limited substitution of (OH) for F.

Comparison of the XRD pattern of AFH with that of β-AlF$_3$ (Table 4) suggests a structural similarity. In this fluoride, sheets of 3- and 6-fold rings of corner-sharing AlF$_6$ octahedra are stacked one above another along the z axis (Le Bail *et al*. 1988). The stacking of these sheets creates hexagonal hollow tubes that are vacant in β-AlF$_3$ (Le Bail *et al*. 1988), but apparently contain H$_2$O in AFH (this study) and in a structurally related phase, β-AlF$_3$•H$_2$O (Grobelny 1977). The phase β-AlF$_3$ appears to be hexagonal owing to cyclic twinning (rotation of 120° around the c axis), but the true symmetry is orthorhombic with space group *Cmcm* (Le Bail *et al*. 1988). In AlF$_2$(OH), two hydroxyl groups replace F in each octahedron (P.H. Ribbe, pers. commun.). The

existence of this phase has not been previously reported in the literature.

Phase A

Phase A was synthesized as clear, equant (rhombohedral ?) crystals 0.01–0.05 mm in size. Experimental data are summarized in Tables 3, 5 and 6.

X-ray, index of refraction, and infrared data (Rosenberg 1972) indicate that AlF_3 hydrolyzes with decreasing temperature in the system AlF_3–Al_2O_3–SiO_2–H_2O according to the reaction:

$$AlF_3 + XH_2O = AlF_{3-x}(OH)_x + XHF,$$

because HF is progressively consumed by the formation of SiF_4 (Rosenberg 1992). In the system AlF_3–Al_2O_3–

H_2O–HF, AlF_3 hydrolyzes with *increasing* temperature according to the above reaction resulting in a decrease in d_{220}, which is probably due to H-bonding. The mean index of refraction of OH-bearing AlF_3 increases progressively from 1.379 ± 0.001 for end-member AlF_3 to 1.405 ± 0.002 for $AlF_{3x}(OH)_x$ (*e.g.*, Table 6, 974, 862) with decreasing d_{220} values and increasing temperature. Direct evidence of hydrolysis is provided by the infrared absorption spectrum of *A* after equilibration at 600°C (Table 5, 1072), which shows an OH-stretching band at 3676 cm^{-1} (Fig. 1).

Although AlF_3 appears to hydrolyze with increasing temperature, the value of x in the general formula is known only approximately at present. For the assemblage A + Crn + fluid, at temperatures between 700° and 625°C, d_{220} averages 1.7567 ± 0.0003 Å as compared to 1.7596 ± 0.0002 Å for end-member AlF_3 (this study). These variations were correlated approximately with chemical composition by EMP analysis of *A* (60.0 wt.% F) in sample 1072 (Table 6), assuming a linear relationship between Δ_{220} and weight % F. Using this calibration, the minimum F-content of *A* is approximately 56.3 wt.%, corresponding to the formula $AlF_{2.45}(OH)_{0.55}$. The maximum F-content observed in this study is 65 wt.%

TABLE 4. XRD DATA FOR AFH

	AFH			β-AlF₃*	
hkl	d_{obs} (Å)	I/I_0	*hkl*	d_{obs} (Å)	I/I_0
100	6.02	100	100	6.002	st
002	3.583	80	002	3.563	st
110	3.486	15	110	3.465	st
102	3.078	5	102	3.063	w
200	3.053	35	200	3.001	st
202	2.471	2	112	2.484	w
112	2.305	1	202	2.295	w
210	2.268	1	210	2.266	w
103	2.212	5	103	2.209	w
211	2.914	5	211	2.161	w
300	2.017	10	300	2.001	m
113	1.973	10	-	-	-
-	-	-	212	1.914	m
004	1.786	20	004	1.782	mst
220	1.720	10	220	1.732	mst

* Grobelny (1977).

TABLE 5. EXPERIMENTAL DATA: AFH COEXISTING WITH A AND FLUID

Temp. (°C)	Exp. No. (+ H₂O)	Comp.*	Time (days)	Products** (+ fluid)	A Δ_{220}***
625	803	9:1	4	AFH + Atr	nm
	802	4:1	4	AFH + Atr	nm
	924	9:1	22	AFH + A	nm
600	1072	A	12	A	4.620
	801	9:1	5	AFH + A	4.598
	800	4:1	5	AFH + Atr	nm
	723	A	16	A + AFHtr	4.592
575	818	9:1	10	AFH + A	nm
	900	9:1	48	AFH	-
	790	A	5	A + AFHtr	4.597
550	465	A	3	AFH + A	nm
	637	A	5	A + AFHtr	4.604
500	501	A	12	AFH + A	nm
450	992	A	28	AFH + A	nm

* AlF_3 : $Al(OH)_3$ molar ratio. tr.: X-ray trace.
** A, $AlF_{3-x}(OH)_x$, AFH, $AlF_2(OH)$. *** Δ_{220} [2θ AlF_3 (220) – 2θ std].

TABLE 6. EXPERIMENTAL DATA: AFH OR A COEXISTING WITH Crn OR T*

Temp. (°C)	Exp. No. (+H₂O)	Comp.**	Time (days)	Products (+ fluid)	A Δ_{220}***
750	405	1:4	16	A + Crn	nm
	1004	A	20	A + Crn-m	4.603
700	970	9:1	24	A + Crn	4.609
	974	2:1	24	A + Crn	4.605
	975	4:1	24	A + Crn	4.615
	686	1:4	7	Crn + A	nm
675	831	4:1	6	A + Crn	4.601
	832	9:1	6	A + Crn	4.609
	833	2:1	6	A + Crn	4.597
	834	1:4	6	A + Crn	nm
650	803	9:1	3	AFH + Crn	-
	804	4:1	3	AFH + Crn	-
	861	4:1	14	A + Crn	4.618
	862	9:1	14	A + Crn-m	4.604
	863	2:1	14	A + Crn	4.605
	864	1:4	14	Crn + Am	nm
	1016	A	18	A + Crn	4.616
625	802	4:1	6	AFH + Crn	-
	923	4:1	22	A + AHF	4.616
	924	9:1	22	AFH + A	-
	926	2:1	22	A + Crn-m	4.611
	927	1:4	22	Crn + A	nm
600	811	1:9 10		AFH + T + Crn	-
	786	1:9	21	AFH + Crn	-
	719	1:4	22	AFH + Crn	-
	721	2:1	22	AFH + Crn	-
575	747	1:4	7	AFH + T	-
	739	1:9	13	AFH + T	-
	902	2:1	48	AFH + Crn-m	-
	903	1:4	48	AFH + Crn	-
	905	1:1	48	AFH + Crn	-

* Symbols: A: $AlF_{3-x}(OH)_x$, AFH: $AlF_2(OH)$, T: "tohdite", Crn: corundum, m: microscope only, nm: not measured.
** AlF_3 : $Al(OH)_3$ molar ratio. *** Δ_{220} [2θ AlF_3 (220) – 2θ std].

(Table 3, 1031, 400°C), corresponding to the formula $AlF_{2.97}(OH)_{0.03}$.

Phase T

The phase T, an alumina hydrate synthesized in the AlF_3-poor portion of the system, has been identified on the basis of its XRD pattern (Table 7) as "tohdite", (T) $5Al_2O_3•H_2O$ (Yamaguchi *et al.* 1964a, b) rather than the similar phase akdalaite, $4Al_2O_3•H_2O$ (Shpanov *et al.* 1970). At present, "tohdite" is considered to be an invalid mineral name by the Commission on New Minerals and Mineral Names (CNMMN), International Mineralogical Association. The name akdalaite was substituted for "tohdite" in some publications (*e.g.*, Tilley & Eggleton 1996). However, a mineral likely to be "tohdite" was recently recognized by the CNMMN (Burke & Ferraris 2005). But in the latest turn of events, it has been shown that akdalaite has the same properties as synthetic and natural "tohdite". Inasmuch as the name akdalaite has priority, "tohdite" will be formally discredited (E.A.J. Burke, pers. commun., 2005). Because this latest change in nomenclature has not yet been submitted for publication, the name "tohdite" is retained for the synthetic material described in this paper.

Although X-ray reflections for the two phases are quite similar, weak reflections at 4.61, 3.17, 2.53, 2.07, 1.925, 1.905, 1.667 and 1.471 Å reported for akdalaite are absent both in "tohdite" and in the alumina hydrate synthesized in this study. Furthermore, the H_2O content determined by weight loss in this study is 3.34% compared to the value 3.41% calculated for "tohdite"; the calculated weight-loss for akdalaite is 4.23%. The IR (OH)-stretching bands of T at 3373 and 3125 cm^{-1} (Fig. 1) are broader and weaker than those for the fluorides.

Phase T crystallized as thin, hexagonal plates up to a few μm in thickness and 100 μm in diameter. In some experiments, it also occurs as well-formed, lath-shaped to acicular crystals with a low birefringence and parallel extinction. At 575°C, phase T appears in experiments of short duration (*i.e.*, one week); in experiments of longer duration, T is replaced progressively by corundum, indicating that T is metastable with respect to Crn + H_2O. However, at and below 475°C, T persists in experiments of 93 days duration (Table 2).

Yamaguchi *et al.* (1964a) synthesized T using AlF_3 as a "mineralizer", but they were also successful in synthesizing "tohdite" in the presence of trace amounts of titanium sulfate. Phase T appears to correspond to phases synthesized by Torkar (1960) and by Aramaki & Roy (1963) from F-free compositions. Phase T occurs naturally in Australian bauxite deposits (Tilley & Eggleston 1994).

Corundum

Corundum (Crn) crystallized as small (1–10 μm), anhedral crystals and larger flat hexagonal plates, not unlike those of T.

Diaspore

Diaspore (Dsp) appeared in place of Crn or T in experiments of long duration at 400°C (Table 2).

Fluid phase

No attempt was made to determine the composition of the fluid phase after the experiments. However, approximate measurements of quench pH were obtained for selected samples using a micro combination electrode. Values of pH for experiments with AlF_3-rich starting compositions (*i.e.*, 9/1, 3/1) were invariably between 1 and 3. AlF_3-poor starting compositions (*i.e.*, 1/9, 1/4) yielded pH values between 4 and 7. The solubility of corundum in 0.1 m HF solutions at 400°C and 1 kbar suggests the formation of both fluoride and hydroxyfluoride complexes of Al in solution (Zaraisky 1994). These complexes are probably also present in the fluid phase synthesized in the present investigation.

PHASE RELATIONS

Phase assemblages synthesized in this study include AHF + corundum + fluid (Table 2), AHF + fluid (Table 2), AHF + AFH + fluid (Table 3), AHF + A + fluid (Table 5), AFH + A + fluid (Table 5), AFH + Crn + fluid (Table 6), A + Crn + fluid (Table 6) and A + fluid.

Phase relations involving AHF are defined by its unit-cell dimension in various assemblages (Fig. 3).

TABLE 7. XRD DATA FOR "TOHDITE"

hkl	Yamaguchi *et al.* (1964b)		This study	
	d (Å)	I/I_0	d (Å)	I/I_0
100	4.85	10	4.85	5
002	4.38	23	4.37	40
101	4.23	11		
102	3.246	60	3.232	20
110	2.788	12	2.780	5
103	2.500	54	2.498	30
200	2.416	12	2.411	5
112	2.352	77	2.353	60
201	2.329	38	2.332	30
004	2.192	4	2.200	30
202	2.1146	100	2.115	100
203	1.8614	48	1.863	30
122	1.8654	13	1.687	10
105	1.6482	4	1.642	5
204	1.6232	26	1.632	15
123	1.5479	34	1.547	15
302	1.5105	20	1.508	5
006	1.4609	4		
205	1.4190	68	1.418	80
220	1.3939	85	1.396	80

The two-phase area of AHF + fluid is bounded on the low-F side by the assemblage AHF + corundum or "tohdite" + fluid (Table 2). This phase boundary has been approached using the low-F composition 1:4 (Fig. 3, open squares) and the high-F compositions 2:1, 1:1 and 3:1 (Fig. 3, filled circles). The cell dimensions of AHF in assemblages with Crn or T and fluid lie on or close to this phase boundary. The AHF + fluid phase area is bounded on the high-F side by the assemablages AHF + AFH + fluid above about 435°C, and AHF + A + fluid below 435°C (Table 3). This phase boundary was determined by experiments with the compositions 4:1, 9:1 and pure AlF_3. The cell dimensions of AHF in assemblages with AFH or A lie along this phase boundary. These two boundaries converge with increasing temperature and meet at approximately 575°C, the maximum thermal stability of AHF in this study, defining the stability field of AHF + fluid. The assemblages AHF + A and AHF + AlOOH (diaspore or böhmite) have been synthesized in preliminary experiments at temperatures as low as 95°C.

The relationship between cell dimensions and F content (Fig. 2) fixes the assemblage AHF + fluid in composition space. A phase diagram for the join AlF_3–$Al(OH)_3$ (Fig. 4) has been constructed on the basis of estimated compositions of AHF, AFH and AlF_3 and the thermal stabilities of the phase assemblages synthesized in the system AlF_3–Al_2O_3–H_2O–HF. This diagram shows that: 1) The maximum thermal stability of AHF at 2 kbar is about 570°C. AHF decomposes to AFH at higher temperatures. 2) AFH intervenes between AHF and A above 435°C and decomposes to A and corundum above 625°C. 3) AHF, AFH and A have compositional ranges due to the substitution of (OH) for F.

Infrared spectroscopy confirms the presence of (OH) in AHF, AFH and A, and also indicates that considerable amounts of structural H_2O are incorporated in AHF and AFH (Fig. 1) as well as in T.

DISCUSSION AND CONCLUSIONS

The phase AlF_3, with a sublimation temperature of 760°C, may be present as a juvenile constituent in the volcanic gases of many volcanos. It has been inferred to be present in the volcanic plume of Mount Hekla, Iceland (Oskarsson 1981), and it has been tentatively identified in volcanic incrustations from the summit area of Mount Erebus, Antarctica (Keys & Williams 1981, Rosenberg 1988). Anhydrous AlF_3 and its monohydrates such as β-AlF_3•H_2O, which has also been tentatively identified from the summit area of Mt. Erebus (Rosenberg 1988), probably crystallize as sublimates directly from the volcanic plume. Fugacities of HF in the plume may be high enough to prevent the hydrolysis of AlF_3 observed at high temperatures in this study. Thus, high-temperature phases in the system AlF_3–Al_2O_3–H_2O–HF may be quenched and preserved

under the "dry" conditions that exist at the summit. Volcanic gases are quenched rapidly from high temperatures, thus bypassing the stability field of AFH and AHF, which do not crystallize directly by sublimation from the volcanic plume. The liquid phase participates in fumarolic deposition even at temperatures well above 100°C (Stoiber & Rose 1974).

At lower temperatures, AHF is precipitated by reaction of extremely acid (*i.e.*, 0.7 < pH < 1.7, Africano & Bernard 2000) volcanic condensates with wallrocks. Acidification of volcanic condensates is probably promoted by oxidation of reduced sulfur species in the aqueous phase between about 100° and 350°C (Africano & Bernard 2000, Stoiber & Rose 1974). The phase AFH, which appears to be stable between about 435° and 625°C, may not exist in nature because its thermal stability lies above the temperature range of oxidation at fumarolic vents. Furthermore, elevated pressures may be required for its crystallization.

Acidic condensates interact with wallrocks, leaching cations from the primary minerals and glass, leaving only silica (Africano & Bernard 2000). Mineral associations, including ralstonite and AHF, in the altered rock reflect increasing oxidation of the fluid (Africano & Bernard 2000). The phase AHF (and ralstonite) is found in black, altered incrustation zones with pyrite, suggesting that these deposits were formed under lower redox conditions and in zones representing a more oxidized environments (Africano & Bernard 2000).

However, in the Valley of Ten Thousand Smokes, AHF is restricted to orange-red crusts forming the outer zone of fossil fumarole deposits, which contain, among other minerals, hematite, consistent with oxidizing conditions (Keith 1991, Papike *et al*. 1991). Similar

FIG. 3. Variation of unit-cell dimension *a* of AHF with temperature in univariant assemblages AHF + Crn + fluid, open squares (composition 1:4) and filled circles (composition 2:1); AHF + AFH + fluid, filled triangles (compositions 9:1 and 4:1, and AHF + A + fluid, filled squares (compositions A and 9:1). The size of the symbols approximates the estimated error.

FIG. 4.   Phase relations on the join AlF₃–Al(OH)₃. F: fluid phase.

mineral zoning has been observed around volcanic fumaroles in Central America (Stoiber & Rose 1974) and in other localities (*e.g.,* Viramonte *et al*. 1976).

After reaction with volcanic rocks, the acidic solutions are thought to have a pH <5 (Africano & Bernard 2000), within the range of fluids coexisting with AHF + Crn (or T) observed in the present investigation. Values of the ratio F/OH in AHF, which vary considerably in F-rich assemblages, could provide an insight into HF fugacities in the coexisting fluid phase, but such assemblages are rare in nature. The composition of AHF in F-poor assemblages (*i.e.,* AHF + Crn + fluid) is not temperature-sensitive and, therefore, not a very useful indicator of HF fugacities in the coexisting fluid phase.

Ralstonite and AHF usually crystallize at temperatures below 200°C in fumarolic deposits (*e.g.,* Naboko 1957, Birnie & Hall 1974, Viramonte *et al*. 1976). However, higher temperatures (200–300°C) apparently accompanied the crystallization of AHF from hydrothermal solutions during late-stage magmatic or postmagmatic processes (*e.g.,* Naboko 1957, Karup-Møller 1973). Thus, in nature, AHF (and ralstonite) crystallize at temperatures well below the range of this study. Nevertheless, phase relations at and above 400°C, which are in accord with those inferred from natural environments, persist qualitatively to temperatures at least as low as 95°C.

ACKNOWLEDGEMENTS

REFERENCES

AFRICANO, F. & BERNARD, A. (2000): Acid alteration in the fumarolic environment of Usu volcano, Hokkaido, Japan. *J. Volcanol. Geotherm. Res.* **97**, 475-495.

ARAMAKI, S. & ROY, R. (1963): A new polymorph of Al₂SiO₅ and further studies in the system Al₂O₃–SiO₂–H₂O. *Am. Mineral.* **48**, 1322-1347.

BIRNIE, R.W. & HALL, J.H. (1974): The geochemistry of El Misti volcano, Peru fumaroles. *Bull. Volcanol.* **38**, 1-15.

BURKE, E.A.J. & FERRARIS, G. (2005): New minerals and nomenclature modifications approved in 2004 by the Commission on New Minerals and Mineral Names, International Mineralogical Association. *Can. Mineral.* **43**, 829-835.

CAROBBI, G. & CIPRIANI, C. (1951): Richerche su alcuni prodotti delle fumarole vesuviane. *Rend. Soc. Ital. Mineral. Petrol.* **7**, 43-44.

COWLEY, J.M. & SCOTT, T.R. (1948): Basic fluorides of aluminum. *J. Am. Chem. Soc.* **70**, 105-109.

DESBOROUGH, G.A. & ROSTAD, O. (1980): Hydrated aluminum hydroxy-fluoride, a ralstonite-like mineral at Big Southern Butte, Snake River Plain, Idaho. *Am. Mineral.* **65**, 1057-1058.

DI GIROLAMO, P. & FRANCO, E. (1968): Ralstonite nelle fratture fumarolizzate del tufo campano di S. Prisco (Caseria). *Atti Accad. Sci. Fis. Mat. Napoli* **7**, 1-18.

EFFENBERGER, H. & KLUGER, F. (1984): Ralstonit: ein Beitrag zur Kenntnis von Zusammensetzung und Kristallstruktur. *Neues Jahrb. Mineral., Monatsh.*, 97-108.

GROBELNY, M. (1977): High temperature crystallization of aluminum fluoride: course, hydrolysis, solid phases. *J. Fluorine Chem*. **9**, 187-207.

HEINRICH, E.W. (1977): Aluminofluoride minerals of the Goldie carbonatite, Fremont County, Colorado. *Mountain Geol*. **14**, 33-46.

HITCHON, B., HOLLOWAY, L.R. & BAYLISS, P. (1976): Formation of ralstonite during low-temperature acid digestion of shales. *Can. Mineral*. **14**, 391-392.

JAMBOR, J.L. & BURKE, E.A.J. (1989): New mineral names. *Am. Mineral*. **74**, 1399-1404.

JAMBOR, J.L., SABINA, A.P,, RAMIK, R.A. & STURMAN, B.D. (1990): A fluorine-bearing gibbsite-like mineral from Francon quarry, Montreal, Quebec. *Can. Mineral*. **28**, 147-153.

KARUP-MØLLER, S. (1973): A gustavite–cosalite–galena-bearing mineral suite from the cryolite deposit at Ivigtut, south Greenland. *Medd. Gronl*. **195**(5).

KEARNS, L.E. (1995): Alumino-fluorides from the Morefield pegmatite, Amelia County Virginia. *Mineral. Rec*. **26**, 551-556.

KEITH, T.E.C. (1991): Fossil and active fumaroles in the 1912 eruptive deposits, Valley of Ten Thousand Smokes, Alaska. *J. Volcanol. Geotherm Res*. **45**, 227-254.

KEYS, J.R. & WILLIAMS, K. (1981): Origin of crystalline, cold desert salts in the McMurdo region, Antarctica. *Geochim. Cosmochim. Acta* **45**, 2299-2309.

LE BAIL, A., JACOBONI, C., LEBLANC, M., DE PAPE, R., DUROY, H. & FOURQUET, J.L. (1988): Crystal structure of the metastable form of aluminum trifluoride, β-AlF$_3$ and the gallium and indium homologs. *J. Solid State Chem*. **77**, 96-101.

MENZ, D.H., MENSING, C., HONLE, W. & VON SCHNERING, H.G. (1992): The thermal behavior of aluminum fluoride–hydroxide hydrate, AlF$_{2.3}$(OH)$_{0.7}$(H$_2$O). *Z. Anorg. Allgem. Chem*. **611**, 107-113.

NABOKO, S.I. (1957): A case of gaseous fluorine metasomatism at an active volcano. *Geochemistry*, 452-455.

NAUGHTON, J.J., GREENBERG, V.A. & GOGUEL, R. (1976): Incrustations and fumarolic condensates at Kilauea volcano, Hawaii: field, drill hole and laboratory observations. *J. Volcanol. Geotherm. Res*. **1**,149-165.

OSKARSSON, N. (1981): The chemistry of Icelandic lava incrustations and the latest stage of degassing. *J. Volcanol. Geotherm. Res*. **10**, 93-111.

PABST, A. (1939): Formula and structure of ralstonite. *Am. Mineral*. **24**, 566-576.

PAPIKE, J.J., KEITH, T.E.C., SPILDE, M.N., GALBREATH, K.C., SHEARER, C.K. & LAUL, J.C. (1991): Geochemistry and mineralogy of fumarolic deposits, Valley of Ten Thousand Smokes, Alaska: bulk chemical and mineralogical evolution of dacite-rich protolith. *Am. Mineral*. **76**, 1662-1673.

PAULY, H. (1965): Ralstonite from Ivigtut, South Greenland. *Am. Mineral*. **50**, 1851-1864.

RAADE, G. & HAUG, J. (1980): Rare fluorides from a soda granite in the Oslo region, Norway. *Mineral. Rec*. **11**, 83-91.

ROBERSON, C.E. & HEM, J.D. (1968): Activity product constant of cryolite at 25°C and one atmosphere using selective-ion electrodes to estimate sodium and fluoride activities. *Geochim. Cosmochim. Acta* **32**, 1343-1351.

ROSENBERG, P.E. (1972): Compositional variations in synthetic topaz. *Am. Mineral*. **57**, 169-187.

ROSENBERG, P.E. (1988): Aluminum fluoride hydrates, volcanogenic salts from Mount Erebus, Antarctica. *Am. Mineral*. **73**, 855-860.

ROSENBERG, P.E. (1990): Stability relations of ralstonite in the system aluminum fluoride–aluminum oxide–water. *Geol. Soc. Am., Abstr. Programs* **22**, 340.

ROSENBERG, P.E. (1992): The hydroxylation of fluorite under hydrothermal conditions. *Can. Mineral*. **30**, 457-462.

SERAFIMOVA, E.K. (1997): Fluorides deposited during post-eruptive activities on Kamchatkan volcanoes. *Volcanol. Seismol*. **18**, 571-614.

SHPANOV, E.P., SIDORENKO, G.A. & STOLYAROVA, T.I. (1970): Akdalaite, a new hydrous modification of alumina. *Zap. Vses. Mineral. Obshchest*. **99**, 333-339 (in Russ.).

STOIBER, R.E. & ROSE, W.I., JR. (1974): Fumarole incrustations at active Central American volcanoes. *Geochim. Cosmochim. Acta* **38**, 495-516.

TILLEY, D.B. & EGGLETON, R.A. (1994): Tohdite (5Al$_2$O$_3$•H$_2$O) in bauxites from northern Australia. *Clays Clay Minerals* **42**, 485-488.

TILLEY, D.B.& EGGLETON, R.A. (1996): The natural occurrence of eta-alumina (eta-Al$_2$O$_3$) in bauxite. *Clays Clay Minerals* **44**, 658-644.

TORKAR, K. (1960): Untersuchungen über Aluminumhydroxyde and –oxyde, **4**. Mitteilung: Beschreibung zweier neuer Aluminiumoxydformen, die bei hydrothermaler Zersetzung von metallischem Aluminium gefunden wurden. *Monatsh. Chem*. **91**, 658-668.

VIRAMONTE, J.G., SUREDA, R.J., BOSSI, G.E., FOURCADE, N.H. & OMARINI, R.H. (1976): Geochemical and mineralogical study of the high temperature fumaroles from Deception Island, South Shetland, Antarctica. *In* Andean and Antarctic Volcanology Problems, Symp. Proc. (O. Gonzales Ferran, ed.). Francesco Giannini and Figli, Napoli, Italy (543-561).

YAMAGUCHI, G., YANAGIDA, H. & SHUITIRO, O. (1964a): A new alumina hydrate, "tohdite" (5Al$_2$O$_3$•H$_2$O). *Bull. Chem. Soc. Japan* **37**, 752-754.

YAMAGUCHI, G. YANAGIDA, H. & SHUITIRO, O. (1964b): The crystal structure of tohdite. *Bull. Chem. Soc. Japan* **37**, 1555-1557.

ZARAISKY, G.P. (1994): The influence of acidic fluoride and chloride solutions on the geochemical behaviour of Al, Si and W. *In* Fluids in the Crust: Equilibrium and Transport Properties (K.I. Shmulovich, B.W.D. Yardley & G.G. Gonchar, eds.). Chapman Hall, London, U.K. (139-162).